Transient and Steady-State Characteristics of DC Machines Fed By Solar Cells

Mohammad S. Widyan, A. Al Tarabsheh, Issa Etier
The Hashemite University, Electrical Engineering Department, 13115 Zarqa, Jordan.
mohammadwidyan@yahoo.com

This paper presents dynamical model and analysis of DC shunt and series motors fed by photovoltaic PV energy systems. The maximum power point of current/voltage I/V characteristics of the PV modules is chosen to be at the rated conditions of the machines. The nonlinear behavior of I/V characteristics of the PV modules and that of the magnetization curve of the ferromagnetic materials of the DC machines are approximated by polynomial curve fitting. The dynamical analysis of the two machines fed by fixed terminal voltage has also been carried out. A comparison between the two cases is outlined. The steady-state output characteristics, the torque-speed characteristics, of the two DC motors with the two inputs are presented and compared. All of the simulations are executed using MATLAB environment.

INTRODUCTION

DC motors are electrical machines that consume DC electrical power and produce mechanical torque. Historically, DC machines are classified according to the connection of the field circuit with respect to the armature circuit. In shunt machines, the field circuit is connected in parallel with the armature circuit while DC series machines have the field circuit in series with the armature where both field and armature currents are identical.

The use of PV systems as a power source for DC machines can be considered a promising area in photovoltaic applications due to the ongoing growth of PV-market. PV arrays comprise several parallel/series connected modules to provide a sufficiently high output voltage for operating common loads and devices. PV modules, on the other hand, consist of parallel/series-connected solar cells [1].

This paper deals with the dynamical modeling and analysis of DC shunt and series motors fed by photovoltaic cells. The maximum power point of the photovoltaic cells are designed to be on rated conditions of the machines. The nonlinearity of the magnetization curve of the ferromagnetic materials of the machines and that of the output characteristics of the photovoltaic cells

are included by polynomial curve fitting. All simulations are carried out using MATLAB.

DYNAMICAL MODEL OF DC SHUNT AND SERIES MOTORS

This section presents the dynamical model of the DC shunt and series motors including the nonlinearity of the magnetization curve of the ferromagnetic materials.

a) DC Shunt Motor

In shunt machine, the field circuit is connected in parallel with the armature circuit. It has the following equivalent circuit:

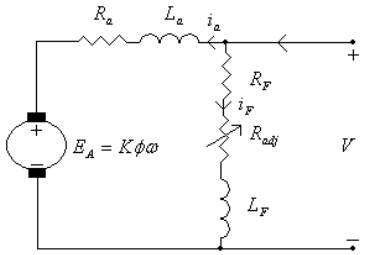

Fig. 1. Equivalent Circuit of DC Shunt Motor

The equation of the field circuit:

$$L_F \frac{di_F}{dt} = V - (R_F + R_{adj})i_F \quad (1)$$

where L_F: field winding inductance, i_F: field current, V: terminal voltage and $R_F + R_{adj}$: field winding resistance.

The equation of the armature circuit:

$$L_a \frac{di_a}{dt} = V - R_a i_a - K\phi\omega \quad (2)$$

where L_a: armature winding inductance, i_a: armature current, R_a: armature resistance, K: constant related to the design of the machine, ϕ: flux per pole of the machine and ω: rotational speed of the machine. The motion equation of the motor is:

$$J \frac{d\omega}{dt} = K\phi i_a - T_L \quad (3)$$

where J: rotor and load moment of inertia and T_L: load torque.

The magnetization curve is the relation between the flux ϕ and the field current i_F. However, it is usually obtained experimentally in terms of the induced voltage $E_A = K\phi\omega$ as function of i_F at a certain rotational speed ω at no load. In this paper, $K\phi$ is expressed as function of the field current i_F based on the data given in [Dynamic Sim. Of El. Mach] after dividing the induced voltage $E_A = K\phi\omega$ by the given rotational speed. $K\phi$ as function of i_F has then been polynomial fitted using the MATLAB instruction 'polyfit'. It is found that the following second order polynomial is accurate enough to represent them at a rotational speed of 2000rpm:

$$K\phi = -0.3084 i_F^2 + 1.0272 i_F + 0.0049 \quad (4)$$

Substituting for $K\phi$ in Eq. (2) yields:

$$L_a \frac{di_a}{dt} = V - R_a i_a + (0.3084 i_F^2 - 1.0272 i_F - 0.0049)\omega \quad (5)$$

and for $K\phi$ in Eq. (3) yields:

$$J \frac{d\omega}{dt} = (-0.3084 i_F^2 + 1.0272 i_F + 0.0049) i_a - T_L \quad (6)$$

b) DC Series Motor

In series machine, the field circuit is connected in series with the armature and therefore the armature and field currents are the same. The equivalent circuit of a DC series motor is:

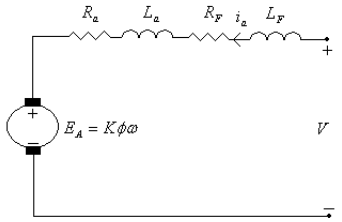

Fig. 2. Equivalent Circuit of DC Series Motor

The equation of the armature:

$$(L_F + L_a)\frac{di_a}{dt} = V - (R_a + R_F) i_a - K\phi\omega \quad (7)$$

where L_F: field winding inductance, L_a: armature winding inductance, i_a: armature current, V: applied terminal voltage, R_a: armature winding resistance, R_F: field winding resistance, K: constant depends of the design of the machine, ϕ: flux per pole and ω: rotational speed of the rotor.

The motion equation:

$$J\frac{d\omega}{dt} = K\phi i_a - T_L \qquad (8)$$

where J : rotor and load moment of inertia and T_L : load torque.

Based on the data presented in [Dynamic sim. Of El. Mach.] and using the MATLAB instruction 'polyfit', it is found that $K\phi$, instead of $K\phi\omega$, can be expressed as function of i_a at a rotational speed of 1200rpm as:

$$K\phi = -0.0017i_a^2 + 0.0938i_a + 0.0062 \qquad (9)$$

Substituting for $K\phi$ in Eq. (7) yields:

$$(L_F + L_a)\frac{di_a}{dt} = V - (R_a + R_F)i_a - (-0.0017i_a^2 + 0.0938i_a + 0.0062)\omega \qquad (10)$$

and for $K\phi$ in Eq. (8) yields:

$$J\frac{d\omega}{dt} = (-0.0017i_a^2 + 0.0938i_a + 0.0062)i_a - T_L \qquad (11)$$

The complete numerical parameters of the DC shunt and series motors are given in appendix A.

PHOTOVOLTAIC CELLS DESIGN AND MAIN CHARACTERISTICS

Figure1,(a) shows an example of a commercial amorphous silicon (a-Si:H) PV module in which twelve single *p-i-n* cells are incorporated. Fig.1,(b) presents the equivalent circuit generally applied for photovoltaic modules; it consists of 12 current sources $I_{ph_i}(1 \le i \le 12)$ in parallel to 12 diodes. Including the resistive elements R_{s_i} and R_{p_i} in the circuit of Fig.1,(b) represents very well the behaviour of real solar cells [1] s a simplification, the PV module is represented as a symbol shown in Fig.1,(c). The specifications of this module are listed in Table 1.

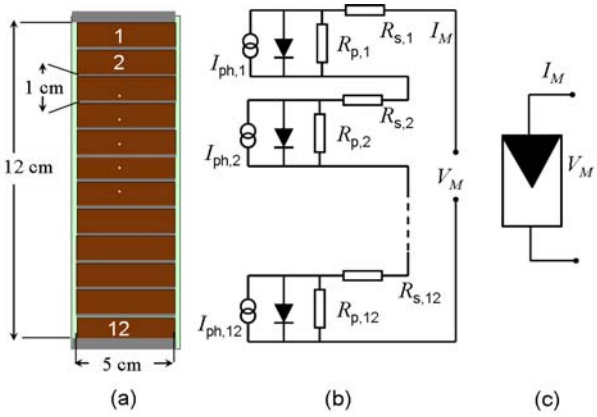

Fig. 1: Thin film amorphous silicon a-Si:H PV module consisting of 12 series-connected solar cells (a) and its equivalent circuit (b). For simplification, the symbol in (c) is used to represents the PV module. The effective area of the module is $60\,cm^2$ where the area of each cell is $5\,cm^2$.

Table 1: Specifications of the PV module shown in Figure 1

Technology	**Amorphous Silicon**
Nominal Power (mW)	431
Voltage at max power (V)	6.78
Current at max power (mA)	63.55
Short circuit current (mA)	74.2
Open circuit voltage (V)	9.15
Dimensions (cm^2)	5×12

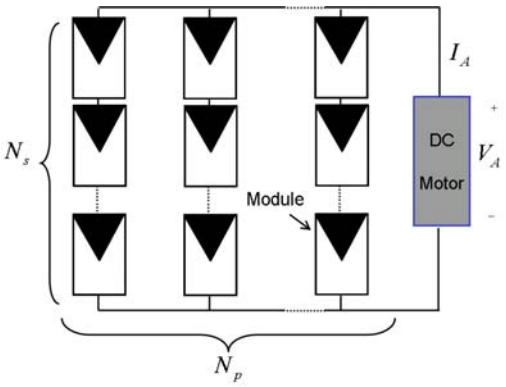

Fig. 2: A PV array consisting of N_s series- and N_p parallel-connected modules loaded by either dc motor shunt or series motor

The *I/V*- characteristics of the PV module are expressed as:

$$I_M = I_0 \exp\left\{\frac{V_M - I_M R_s}{n_M V_t} - 1\right\} + \frac{V_M - I_M R_s}{R_p} - I_{phM} \quad (12)$$

where I_M is the output current of the module, I_0 is the reverse-saturation current, V_M is the output voltage of the module, R_s is the series resistance per module, n is the ideality factor per module, V_t is the thermal voltage and it equals 25.9 mV at T=300K, R_p is the parallel resistance per module and I_{phM} is the generated current per module

Therefore, the relationship between the current and the voltage of a PV array is written as:

$$I_A = N_p \left(I_0 \exp\left\{\frac{\frac{V_A}{N_s} - \frac{I_A}{N_p} R_s}{n_A V_t} - 1\right\} + \frac{\frac{V_A}{N_s} - \frac{I_A}{N_p} R_s}{R_p} - I_{phM} \right) \quad (13)$$

In this paper, the rated conditions of the load are 130V and 16A. To generate this rated values, N_s and N_p should be selected as listed in Table 2.

Table 2: Parameters of the designed PV array

Design Voltage (V)	130
Design Current (A)	16
N_s	19
N_p	252
Area of PV array (m^2)	5.8

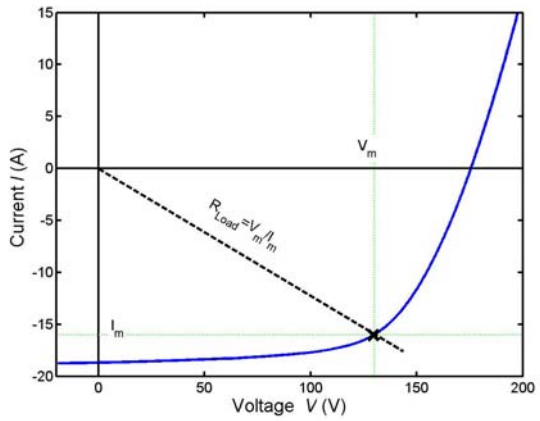

Fig. 3: Current/voltage characteristics of the designed PV array consisting of 19 series- and 252 parallel-connected modules.

Apparently, the output characteristics of the photovoltaic cells are highly nonlinear. It has been curve fitted using the MATLAB instruction "polyfit". For this system, it is found that a polynomial of the 9th order is accurate enough to represent the output voltage as function of the current as:

$$V = -1.352164\times10^{-6} I^9 + 1.077924\times10^{-4} I^8 - 3.592593\times10^{-3} I^7 + 6.485054\times10^{2} I^6 + 0.686478 I^5 + 4.309698 I^4 - 15.453793 I^3 + 28.674508 I^2 - 24.115529 I + 179.975812 \quad (13)$$

where V : the terminal voltage of the photovoltaic cells and I is the output current of the cells.

The terminal voltage V of Eqs. (1), (5) and (10) is replaced by the expression of Eq. (12) when the motors are fed by photovoltaic cells. In shunt motor, I represents $i_F + i_a$ and in series motor I represents i_a.

NUMERICAL SIMULATIONS

The numerical simulations of the DC shunt and series motors are presented in this section. Figure 3 shows the field current of the DC shunt motor after a step change in the load torque from 5Nm to the rated torque of 10.4Nm subjected at t =5s for the two cases of fixed terminal voltage and a terminal voltage supplied by the photovoltaic cells with a field resistance of $100\,\Omega$. When the load increases, the current withdrawn by the motor increases. The terminal voltage of the photovoltaic cell decreases as a result. At light loads, the terminal voltage of the photovoltaic cells is higher than the rated voltage of the machine. This justifies the higher field current at the light load of 5Nm in case of photovoltaic cells. The response of the armature current is shown in Fig. 4 and the corresponding rotational speed is shown in Fig. 5. In all responses, the steady-state values at the rated load torque are in good agreement as the photovoltaic cells are designed to provide the rated voltage at the rated current withdrawn by the motor.

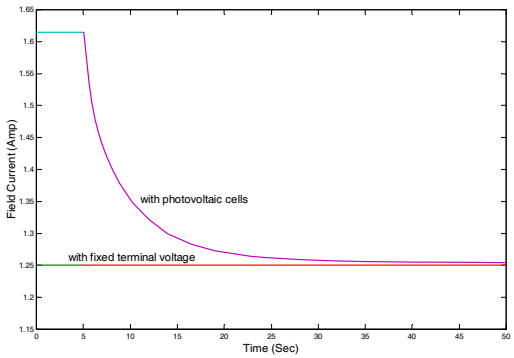

Fig. 3. Field current of DC shunt motor after a step change on the load torque from 5Nm to 10.4Nm with a field resistance of $100\,\Omega$

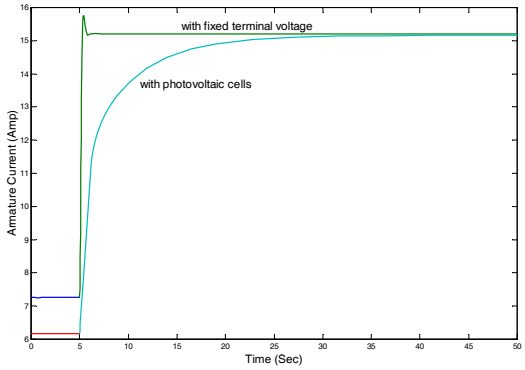

Fig. 4. Armature current of DC shunt motor after a step change on the load torque from 5Nm to 10.4Nm with a field resistance of $100\,\Omega$

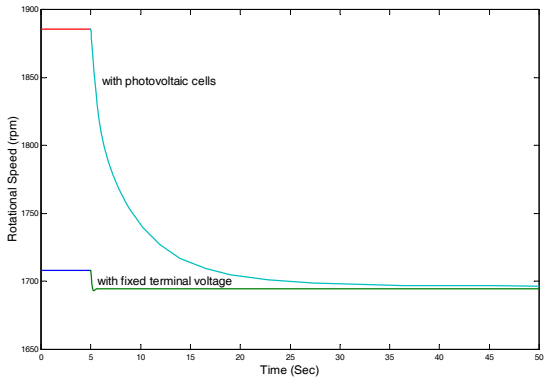

Fig. 5. Rotational speed of DC shunt motor after a step change on the load torque from 5Nm to 10.4Nm with a field resistance of $100\,\Omega$

The simulations executed on the DC shunt motor are repeated for the series motor. Figure 6 shows the armature current of the series motor after a step increase in the load torque from 5Nm to 17Nm for the cases of fixed terminal voltage and a terminal voltage supplied by photovoltaic cells. The steady state armature current in case of photovoltaic cells is slightly higher than that when the motor is fed by fixed terminal voltage and so is the rotational speed as shown in Fig. 7. These small deviations are justified by the small difference in the voltage supplied by the photovoltaic cells compared with the fixed voltage of 125V as shown in Fig. 8. This difference comes as result of the fact that the output voltage of the photovoltaic cells depends on the value of the output current.

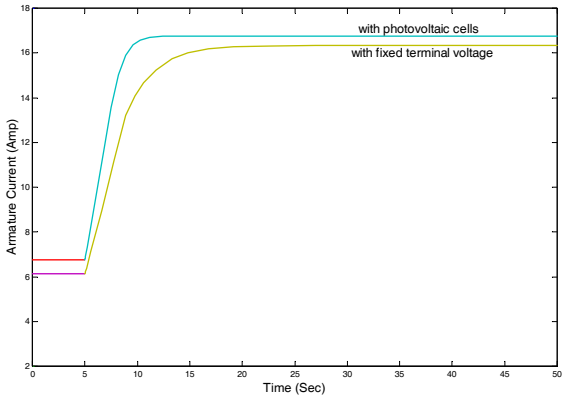

Fig. 6. Armature current of the DC series motor after a step increase in the load torque from 5Nm to 17Nm

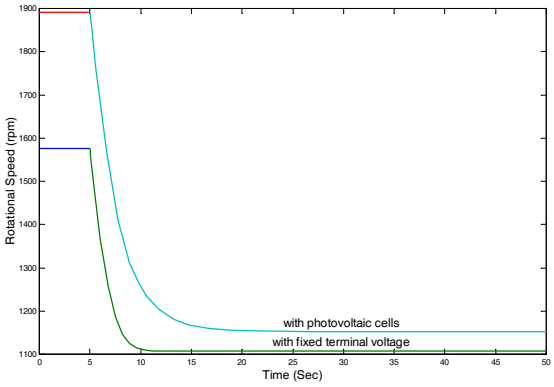

Fig. 7. Rotational speed of the DC series motor after a step increase in the load torque from 5Nm to 17Nm

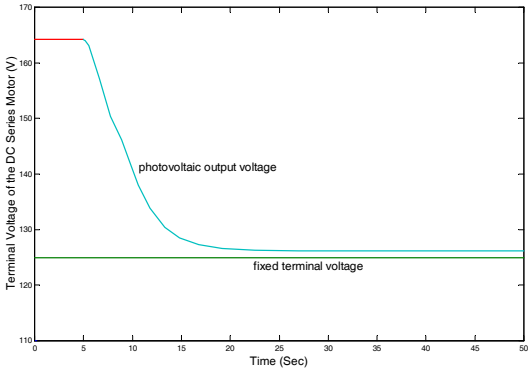

Fig. 8. Terminal voltage of the DC series motor (photovoltaic cells voltage) after a step increase in the load torque from 5Nm to 17Nm compared with the fixed voltage

STEADY-STATE OUTPUT CHARACTERISTICS

The steady-state output characteristics (torque-speed characteristics) of the two motors when fed by both fixed terminal voltage and photovoltaic cells are studied. The operating points of the systems are obtained by dropping out all the time derivative terms of the dynamical differential equations and solving the resulting nonlinear algebraic equations. This has been carried out using the MATLAB Symbolic Math Toolbox instruction 'solve'. Figure 13 shows the torque-speed characteristics of DC shunt motor and Fig. 14 shows that of the DC series motor. Clearly, at the rated load torque the rotational speed of the motors in both cases are in good agreement as the terminal voltage of the photovoltaic cells is very close to the rated voltage supplied in case of fixed terminal voltage. At lighter loads, the speed in case of photovoltaic cells is higher for both motors. This takes place because the terminal voltage of the photovoltaic cells is higher than the fixed voltage as the current withdrawn from the cells is lower at lighter loads.

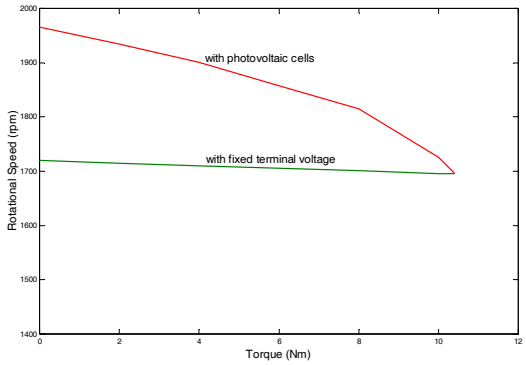

Fig. 13. Torque-speed characteristics of DC shunt motor with photovoltaic cells and fixed terminal voltage

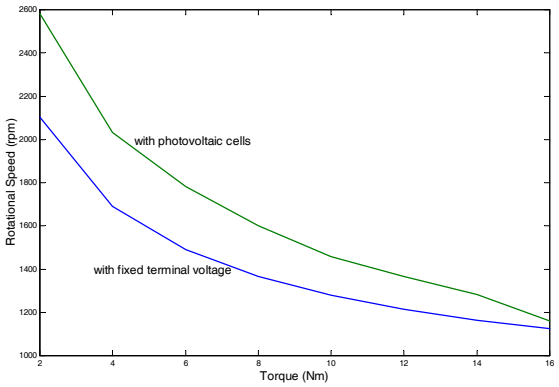

Fig. 14. Torque-speed characteristics of DC series motor with photovoltaic cells and fixed terminal voltage

CONCLUSIONS

The dynamical analysis of DC shunt and series motors fed by photovoltaic cells are studied. The photovoltaic cells are designed to provide the rated voltage of the machine at the machine rated current. The simulation results are compared with the case of fixed terminal voltage. The nonlinearity of the output characteristics of the photovoltaic cells and that of the magnetization curve of the DC machines are included in the simulations by polynomial curve fitting. The results show that when the machine is run at the rated conditions, the steady-state values are in good agreement in both cases of photovoltaic cells and fixed terminal voltage. At light loads with photovoltaic cells, the speed and current of the machine are higher as the voltage supplied is higher. The output steady-state characteristics of the two machines are studied and compared in case of the two inputs. All simulations are carried out using MATLAB environment.

REFERENCES

[1] L. D. Partain, Solar *cells and their applications*, John Wiley & Sons, Inc., p. 164-165, (1995).

[2] J. Merten, M. Asensi, C. Voz, A. V. Shah, R. Platz, and J. Andreu, 'Equivalent Circuit and Analytical Analysis of Amorphousn Silicon Solar Cells and Modules', IEEE Transactions on Electron Devices 45, 423 (1998).

[3] R. M. Swanson, *Handbook of Photovoltaic Science and Engineering*, edited by A. Luque and S. Hegedus (Wiley, West Sussex, England, 2003) p. 102.

APPENDIX A

1) The numerical parameters of the DC shunt motor are:

$L_F = 10\,H$, $R_F + R_{adj} = 100\,\Omega$, $V = 125\text{V}$, $L_a = 18$ mH , $R_a = 0.24\,\Omega$, $J = 0.5\,kgm^2$.

2) The numerical parameters of the DC series motor are:

$L_F = 44\,mH$, $R_F = 0.2\Omega$, $V = 125\text{V}$, $L_a = 18\,mH$, $R_a = 0.24\,\Omega$, $J = 0.5\,kgm^2$.